Wigner crystallization at graphene edges

A. D. Güçlü
Department of Physics, Izmir Institute of Technology, IZTECH, TR-35430, Izmir, Turkey
(Received 30 July 2015; revised manuscript received 21 December 2015; published 12 January 2016)

Using many-body configuration interaction techniques, we show that Wigner crystallization occurs at the zigzag edges of graphene at surprisingly high electronic densities up to 0.8 nm^{-1}. In contrast with one-dimensional electron gas, the flatband structure of the edge states makes the system interaction dominated, facilitating electronic localization. The resulting Wigner crystal manifests itself in pair-correlation functions, and evolves smoothly as the edge electron density is lowered. We also show that the crystallization affects the magnetization of the edges. While the edges are fully polarized when the system is charge neutral (i.e., high density), above the critical density, the spin-spin correlations between neighboring electrons go through a smooth transition from antiferromagnetic to magnetic coupling as the electronic density is lowered.

DOI: 10.1103/PhysRevB.93.045114

I. INTRODUCTION

Wigner crystallization, i.e., localization of electrons induced by electron-electron interactions [1], remains a key issue in strongly interacting systems. In an electron gas, as the electronic density is reduced, the Coulomb repulsion energy overcomes the kinetic energy and the electrons become localized at their classical positions. The two limits, high density Fermi liquid and low density Wigner crystal, are well understood. However, the crossover in between is a complex many-body problem which was previously investigated for various electron gas systems in various dimensions both theoretically [2–13] and experimentally [14–19]. In particular, it is expected that Wigner crystallization has important implications on the transport properties of two-dimensional [14] and one-dimensional [9,12,16–19] systems.

For graphene [20–23], the investigation of Wigner crystallization remains limited [24–27] partially due to the fact that for massless Dirac electrons with a linear dispersion (as opposed to the quadratic dispersion of free electron gas), the interaction strength does not depend on electronic density [28]. It is, however, possible to induce a mass term, for instance, through application of an external magnetic field, for which the Wigner crystal regime was studied within mean-field theory [24,25], or through size quantization [27]. Another situation where Wigner crystallization in graphene may occur is when zigzag edges are present, as suggested in Ref. [26]. However, as far as we know, a detailed analysis of the many-body problem of Wigner crystal transitions at graphene edges is lacking. Indeed, zigzag edges give rise to a band of half-filled degenerate states near the Fermi level without the need for an external magnetic field. Electrons populating these edge states constitute a particularly interesting many-body system since their relative kinetic energy is close to zero, thus the properties are dominated by Coulomb interactions. So far, most of the previous literature on interaction effects due to edge states in various graphene systems focused on magnetic properties [28–41]. In particular, room-temperature magnetic properties of the zigzag edge state in graphene nanoribbons were recently investigated experimentally [42]. However, for the design of carbon-based next-generation devices such as nanoribbons [29–36] and quantum dots [37–41], an in-depth understanding of Wigner crystallization at graphene edges is necessary and a focused investigation of the liquid to crystal crossover is lacking.

In this paper, we use a combination of the tight-binding method and configuration interaction technique on a two-dimensional honeycomb lattice to show that strong Wigner crystallization does indeed occur at the zigzag edges as the electronic density is varied. An analysis of the pair-correlation functions shows that the critical electronic density where the localization occur is close to 0.8 nm^{-1}, a value much higher than the critical density for a one-dimensional (1D) electron gas. Indeed, for the 1D electron gas, the formation of a Wigner crystal was observed using tunneling spectroscopy into a quantum wire, and clear evidence of electron localization was found at a density of $\rho^{1D} \sim 20\ \mu m^{-1}$ [15], whereas quantum Monte Carlo calculations give $\rho^{1D} \sim 15\ \mu m^{-1}$ [12], both significantly lower than the critical density at the graphene edges found in this work. Finally, we investigate ground state magnetization and spin-spin correlation functions between neighboring electrons to show that the spin correlations are strongly tied to the formation of a 1D Wigner crystal as a function of electronic density.

II. MODEL AND METHOD

In order to model the interaction effects at the zigzag edges, we start with a graphene ribbon with a periodic boundary condition [36], consisting of $N_a = 1456$ atoms, with a length of $L = 12.8$ nm and a width of $W = 2.9$ nm. This gives a total of $n_s = 30$ edge states [see Fig. 1(a)], i.e., 15 edge states on each edge, which are computed using the tight-binding technique within the next-nearest-neighbor approximation of p_z orbitals. The nearest-neighbor and next-nearest-neighbor hopping elements are taken to be $t_{nn} = -2.8$ eV and $t_{nnn} = -0.1$ eV [21]. In addition, since our main goal is to investigate the Wigner crystal properties of a single edge, a small electric-field perturbation perpendicular to the edges was added in order to decouple the states belonging to opposite edges. Next, the 15 edge states belonging to the upper edge were used to compute the two-body scattering matrix elements $\langle ps|V|df\rangle$ in terms of the two-body localized p_z orbital scattering matrix elements $\langle ij|V|kl\rangle$. Slater type orbitals [41] were used to calculate the scattering matrix elements. In order to take into account the screening effect by a surrounding medium and

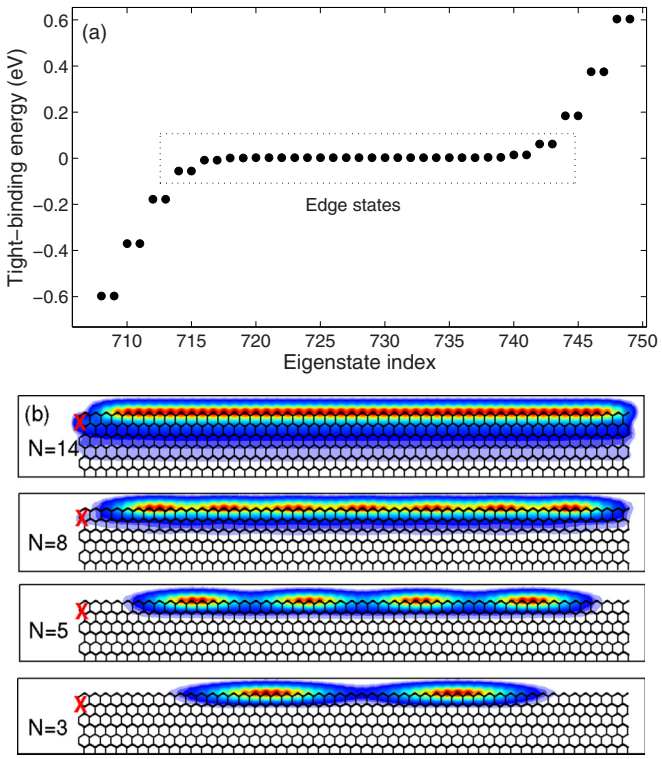

FIG. 1. (a) Tight-binding energy spectrum around the Fermi level within the nearest-neighbor approximation. (b) Two-dimensional pair-correlation functions for $N = 14, 8, 5$, and 3 electrons occupying the zigzag graphene edge. The position of the fixed electron is indicated by a cross (red online). At $N = 14$, charge oscillations only at the atomic level are observed. At lower N values, $N - 1$ peaks arise and become increasingly localized, indicating the formation of a one-dimensional Wigner crystal.

sigma electrons, a dielectric constant of $\kappa = 6$ was used, reducing, for instance, the on-site Coulomb interaction to $U = 2.75$ eV [41]. One should note that, although the edge states are separated from bulk states by an energy gap of the order of 0.1 eV in our model system [see Fig. 1(a)], in the limit of large ribbons the distinction between edge and bulk states becomes blurry and there may be a width dependence on the Wigner crystallization. However, as the edge states are strongly localized at the edges and exponentially decay into the bulk, the wave-function overlap within them is much stronger than their overlap with bulk state wave functions. Therefore, we expect the electronic correlations between the edge and bulk states to be weak. Hence the configuration interaction calculations can be performed in the subspace of edge states. Moreover, the effects of bulk states are present in the model in the mean-field sense. Finally, ground states in subspaces (N, S_z) with different electron numbers N occupying the edge states and z components of the total spin S_z are found using diagonalization of the many-body Hamiltonian given by

$$H_{\mathrm{MB}} = \sum_{s,\sigma} E_s a^\dagger_{s\sigma} a_{s\sigma} + \frac{1}{2} \sum_{\substack{s,p,d,f,\\ \sigma,\sigma'}} \langle sp|V|df\rangle a^\dagger_{s\sigma} a^\dagger_{p\sigma'} a_{d\sigma'} a_{f\sigma}. \quad (1)$$

Here, E_s are the kinetic energies in the nearly degenerate shell of edge states. By comparing the ground state energies of different (N, S_z) subspaces, it is then possible to deduce the ground state total spin S. In this work, the dimension of the largest matrix we have diagonalized using the Lanczos technique is $2\,927\,925 \times 2\,927\,925$.

III. RESULTS

In systems with, e.g., translational or rotational symmetry, electronic localization can be conveniently investigated through pair-correlation functions:

$$P_{\sigma_1\sigma_2}(\mathbf{r}_1, \mathbf{r}_2) = \langle n_{\sigma_1}(\mathbf{r}_1) n_{\sigma_2}(\mathbf{r}_2)\rangle = \sum_{\sigma_3,\ldots,\sigma_N} \int d\mathbf{r}_3 \cdots d\mathbf{r}_N \times |\Psi(\mathbf{r}_1,\sigma_1;\ldots;\mathbf{r}_N,\sigma_N)|^2, \quad (2)$$

which gives the conditional probability to find an electron with spin σ_1 at the position $\mathbf{r}_1$ provided another electron with spin σ_2 is located at $\mathbf{r}_2$. Figure 1(b) shows the pair-correlation functions for different electron numbers N populating the edge states. The fixed electron has spin up and is located at the position indicated by a cross. At $N = 14$, i.e., close to charge neutrality, no charge inhomogeneities (except due to localization over single atoms) is observed. However, when the density is reduced, oscillations start to appear. At $N = 8$, oscillations are weak but seven peaks (not counting the fixed electron) are observed, which is an indication of Wigner crystallization. At lower densities, localization is strongly enhanced and the overlap between the electrons is close to zero.

Although the pair-correlation plots are convenient for the visualization of Wigner crystallization, they do not allow one to quantify the degree of localization and to pinpoint the liquid to crystal crossover. This can be achieved by analyzing the power spectrum [8], i.e., the Fourier transform $F(k)$ of $P_{\sigma\sigma_0}(\mathbf{r}, \mathbf{r}_0)$ in the x direction along the ribbon. In Fig. 2(a), we show $F(k)$ for six and 11 electrons. For six electrons, we clearly see a peak at $k = 6$, a signature of electronic localization at their classical positions [8]. For $N = 11$, however, no localization is observed, indicating that the electronic density is too high to allow for Wigner crystallization. In order to pinpoint the electronic density where the localization occurs, Fig. 2(b) shows the power spectrum peak height $F(k = N)$ for N up to 14. We see that, as the electronic density is decreased, the peak height decreases, indicating a transition toward a liquid state. Above $N = 10$, no localization is observed. In particular, the system is in a liquid state in the vicinity of charge neutrality, i.e., $N = 15$. The crossover value corresponds to a one-dimensional density of 0.8 nm^{-1}. This value is strikingly higher than the critical density for 1D electron gas for which experimental observations [15] and theoretical calculations [12] give $n^{1\mathrm{D}} \sim 15$–$20\ \mu\mathrm{m}^{-1}$. We note, however, that the specific choice of the value of the dielectric constant may affect the value of the critical density found here. The dielectric constant dependence of the critical density requires further investigation.

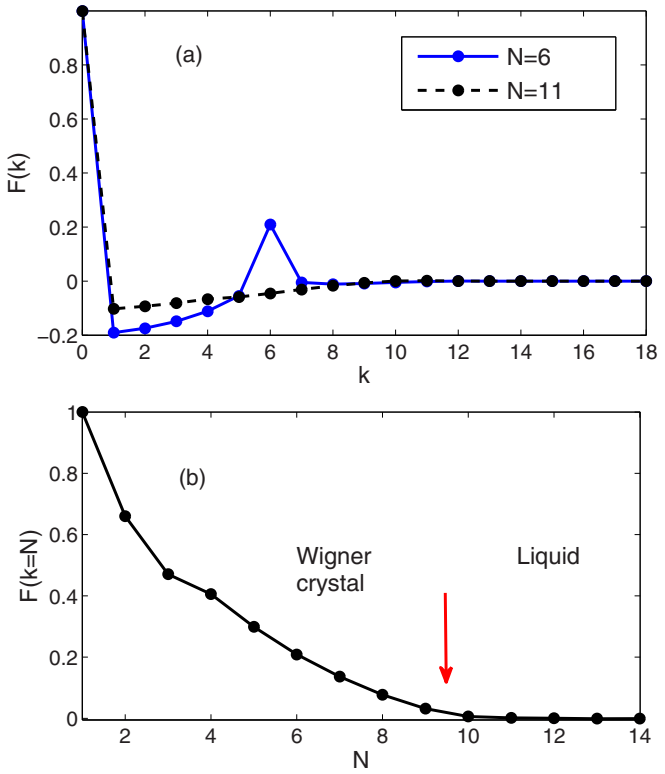

FIG. 2. (a) Power spectrum as a function of Fourier component k for $N = 6$ electrons (solid lines, blue online) and $N = 11$ electrons (dashed lines). For $N = 6$, a peak at $k = 6$ is observed which is an indication of charge localization at classical locations. (b) Power spectrum peak height at $k = N$ as a function of N. Above $N = 10$, the peak height is practically zero, which indicates a lack of Wigner crystallization. The solid-liquid crossover occurs at a one-dimensional density of 0.8 nm^{-1}.

We now analyze the ground state magnetic properties as a function of electronic density. Figure 3(a) shows the ground state total spin S as a function of the number of edge electrons N. It is well established that, in agreement with Lieb's theorem [43], a charge neutral system gives rise to ferromagnetic edges. In our case, this means that for $N = 15$, the total spin is $S_{max} = 15/2$. However, away from charge neutrality, correlation effects are expected to strongly affect the magnetization [36]. In Fig. 3(a), the dashed line shows the maximum possible polarization. The shaded area indicates an uncertainty in S due to computational limitations, since it becomes exponentially more difficult to diagonalize matrices for small values of S_z at large N. Thus, the solid line in this area represents an upper limit to S. However, the uncertainty does not affect our estimation of the critical density of Wigner crystallization since the crystallization is already very weak at these N values. Nevertheless, a clear reduction in magnetization, which is consistent with but more pronounced than in previous calculations for smaller system sizes [32], is observed. In Figs. 3(b)–3(d), we also investigate the spin dependence of the power spectra for $N = 8$, 9, and 10. For the fully polarized state, $S = N/2$, the power spectrum peak height is found to be always higher than the depolarized ground state, indicating stronger localization. However, the difference

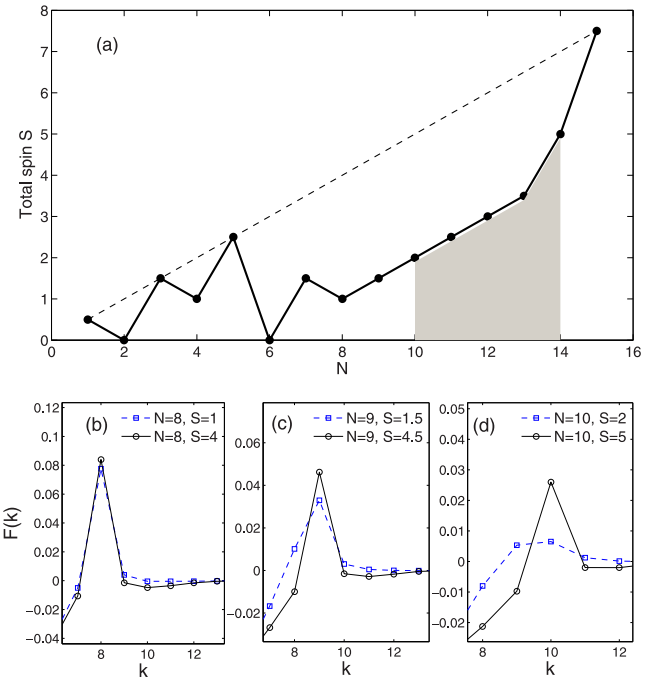

FIG. 3. (a) Ground state total spin S as a function of the number of edge electrons N. The dashed line shows the maximum possible total spin and the shaded area indicates the uncertainty in the total spin due to computational limitations. At $N = 15$, the system is charge neutral and the edges are fully polarized. Away from charge neutrality, a reduction in magnetization occurs. (b)–(d) Spin dependence of the power spectra for $N = 8$, 9, and 10.

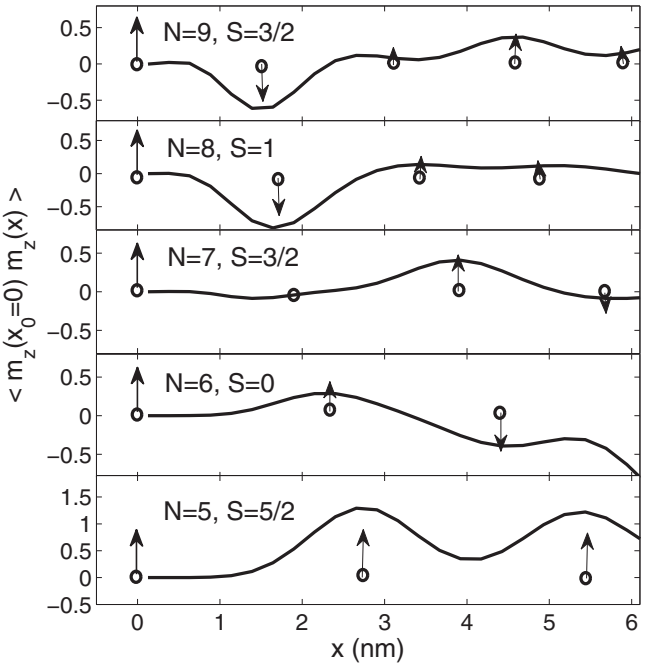

FIG. 4. Ground state spin-spin correlation function along the graphene edge for $N = 9, 8, 7, 6$, and 5. The small circles with arrows represent the classical position of the localized electrons and their effective spin relative to the fixed electron at $x = 0$. As the density is lowered, the magnetic correlation between the nearest neighbors switches from antiferromagnetic coupling to ferromagnetic coupling. The vertical scale is kept the same in all panels.

becomes negligible below $N = 9$, which is another indication that the system enters the Wigner crystal regime [8].

In order to investigate further the connection between the Wigner crystallization and the ground magnetization, in Fig. 4 we plot the ground state spin-spin correlation functions $\langle m_z(x_0)m_z(x)\rangle$ along the edge atoms, where $m_z = n_\uparrow - n_\downarrow$. The small circles with arrows represent the classical position of the localized electrons and their effective spin relative to the fixed electron at $x = 0$. For $N = 9$, Wigner localization has already started but it is weak, with a ground state total spin of $S = 3/2$. The spin-spin correlation function at the nearest neighbors is negative, indicating antiferromagnetic coupling. For $N = 8$, the spin-spin correlation function does not change significantly compared to the $N = 9$ case. However, as the electronic density is decreased further, the average distance between the electrons increases faster, and the magnetic correlations are affected accordingly. As a result, for $N = 7$ and $S = 3/2$, the magnetic correlations between the nearest electrons drop significantly, and become ferromagnetic for $N = 6$ and $S = 0$. This ferromagnetic coupling between the nearest electrons is further enhanced for $N = 5$ and $S = 5/2$. These results show that the magnetization of the edges is closely tied to the evolution of the Wigner crystallization.

IV. CONCLUSION

To conclude, we have shown that a one-dimensional Wigner crystallization occurs at the zigzag edges of graphene. An analysis of pair-correlation functions through configuration interaction calculations indicates that the crossover from the Fermi liquid to Wigner solid occurs near a strikingly high critical density of $0.8\ \mathrm{nm}^{-1}$, as compared to the critical density $n^{1D} \sim 15$–$20\ \mu\mathrm{m}^{-1}$ for the one-dimensional electron gas. While the spin of the ground state of the charge neutral system is fully polarized, we observe magnetic depolarization and oscillations as the liquid-solid crossover occurs. By analyzing the spin-spin correlations between the neighboring electrons, we have shown that the magnetic oscillations are accompanied by a transition from antiferromagnetic to ferromagnetic coupling between the localized electrons. Localization effects can be observed, for instance, using tunneling spectroscopy measurements, as was done for a one-dimensional electron gas [17]. Clearly, for the design of carbon-based spintronic devices, Wigner crystallization must be taken into account for a full understanding of charge and spin transports. Finally, we note that although we have considered an ideal edge without any structural imperfections, inhomogeneities are expected to amplify and not wash out the liquid to crystal transition [6]. Thus, in more realistic graphene structures, Wigner crystallization should be even more robust, strongly affecting both the transport and spin properties. Identification of the combined effects of imperfections and interaction induced localization requires further investigations.

ACKNOWLEDGMENTS

This work was supported by The Scientific and Technological Research Council of Turkey (TUBITAK) under the 1001 Grant Project No. 114F331 and by Bilim Akademisi–The Science Academy, Turkey under the BAGEP program. The author thanks Pawel Hawrylak, Harold U. Baranger, and Nejat Bulut for valuable discussions.

[1] E. Wigner, Phys. Rev. **46**, 1002 (1934).
[2] B. Tanatar and D. M. Ceperley, Phys. Rev. B **39**, 5005 (1989).
[3] A. V. Filinov, M. Bonitz, and Yu. E. Lozovik, Phys. Rev. Lett. **86**, 3851 (2001).
[4] C. Attaccalite, S. Moroni, P. Gori-Giorgi, and G. B. Bachelet, Phys. Rev. Lett. **88**, 256601 (2002).
[5] X. Waintal, Phys. Rev. B **73**, 075417 (2006).
[6] A. Ghosal, A. D. Güçlü, C. J. Umrigar, D. Ullmo, and H. U. Baranger, Nat. Phys. **2**, 336 (2006).
[7] A. Ghosal, A. D. Güçlü, C. J. Umrigar, D. Ullmo, and H. U. Baranger, Phys. Rev. B **76**, 085341 (2007).
[8] A. D. Güçlü, A. Ghosal, C. J. Umrigar, and H. U. Baranger, Phys. Rev. B **77**, 041301(R) (2008).
[9] K. A. Matveev, Phys. Rev. B **70**, 245319 (2004).
[10] M. Casula, S. Sorella, and G. Senatore, Phys. Rev. B **74**, 245427 (2006).
[11] L. Shulenburger, M. Casula, G. Senatore, and R. M. Martin, Phys. Rev. B **78**, 165303 (2008).
[12] A. D. Güçlü, C. J. Umrigar, H. Jiang, and H. U. Baranger, Phys. Rev. B **80**, 201302(R) (2009).
[13] A. C. Mehta, C. J. Umrigar, J. S. Meyer, and H. U. Baranger, Phys. Rev. Lett. **110**, 246802 (2013).
[14] S. V. Kravchenko and M. P. Sarachik, Rep. Prog. Phys. **67**, 1 (2004).
[15] H. Steinberg, O. M. Auslaender, A. Yacoby, J. Qian, G. A. Fiete, Y. Tserkovnyak, B. I. Halperin, K. W. Baldwin, L. N. Pfeiffer, and K. W. West, Phys. Rev. B **73**, 113307 (2006).
[16] O. M. Auslaender, A. Yacoby, R. de Picciotto, K. W. Baldwin, L. N. Pfeiffer, and K. W. West, Science **295**, 825 (2002).
[17] O. M. Auslaender, H. Steinberg, A. Yacoby, Y. Tserkovnyak, B. I. Halperin, K. W. Baldwin, L. N. Pfeiffer, and K. W. West, Science **308**, 88 (2005).
[18] V. V. Deshpande and M. Bockrath, Nat. Phys. **4**, 314 (2008).
[19] B. Brun, F. Martins, S. Faniel, B. Hackens, G. Bachelier, A. Cavanna, C. Ulysse, A. Ouerghi, U. Gennser, D. Mailly, S. Huant, V. Bayot, M. Sanquer, and H. Sellier, Nat. Commun. **5**, 4290 (2014).
[20] P. R. Wallace, Phys. Rev. **71**, 622 (1947).
[21] A. H. C. Neto, F. Guinea, N. M. R. Peres, K. S. Novoselov, and A. K. Geim, Rev. Mod. Phys. **81**, 109 (2009).
[22] K. S. Novoselov, A. K. Geim, S. V. Morozov, D. Jiang, Y. Zhang, S. V. Dubonos, I. V. Grigorieva, and A. A. Firsov, Science **306**, 666 (2004).
[23] Y. B. Zhang, Y. W. Tan, H. L. Stormer, and P. Kim, Nature (London) **438**, 201 (2005).
[24] C.-H. Zhang and Y. N. Joglekar, Phys. Rev. B **75**, 245414 (2007).
[25] R. Côté, J.-F. Jobidon, and H. A. Fertig, Phys. Rev. B **78**, 085309 (2008).
[26] H. Wang and V. W. Scarola, Phys. Rev. B **85**, 075438 (2012).

[27] K. A. Guerrero-Becerra and M. Rontani, Phys. Rev. B **90**, 125446 (2014).
[28] A. D. Güçlü, P. Potasz, M. Korkusinski, and P. Hawrylak, *Graphene Quantum Dots* (Springer, Berlin, 2014).
[29] K. Wakabayashi, M. Sigrist, and M. Fujita, J. Phys. Soc. Jpn. **67**, 2089 (1998).
[30] Y.-W. Son, M. L. Cohen, and S. G. Louie, Nature (London) **444**, 347 (2006).
[31] O. V. Yazyev and M. I. Katsnelson, Phys. Rev. Lett. **100**, 047209 (2008).
[32] B. Wunsch, T. Stauber, F. Sols, and F. Guinea, Phys. Rev. Lett. **101**, 036803 (2008).
[33] J. Jung and A. H. MacDonald, Phys. Rev. B **79**, 235433 (2009).
[34] M. Wimmer, I. Adagideli, S. Berber, D. Tomanek, and K. Richter, Phys. Rev. Lett. **100**, 177207 (2008).
[35] O. V. Yazyev, R. B. Capaz, and S. G. Louie, Phys. Rev. B **84**, 115406 (2011).
[36] A. D. Güçlü, M. Grabowski, and P. Hawrylak, Phys. Rev. B **87**, 035435 (2013).
[37] M. Ezawa, Phys. Rev. B **76**, 245415 (2007).
[38] J. Fernandez-Rossier and J. J. Palacios, Phys. Rev. Lett. **99**, 177204 (2007).
[39] W. L. Wang, S. Meng, and E. Kaxiras, Nano Lett. **8**, 241 (2008).
[40] A. D. Güçlü, P. Potasz, O. Voznyy, M. Korkusinski, and P. Hawrylak, Phys. Rev. Lett. **103**, 246805 (2009).
[41] P. Potasz, A. D. Güçlü, A. Wojs, and P. Hawrylak, Phys. Rev. B **85**, 075431 (2012).
[42] G. Z. Magda, X. Jin, I. Hagymasi, P. Vancso, Z. Osvath, P. Nemes-Incze, C. Hwang, L. P. Biro, and L. Tapaszto, Nature (London) **514**, 608 (2014).
[43] E. H. Lieb, Phys. Rev. Lett. **62**, 1201 (1989).